



This is a repository copy of *Direct normal form analysis of oscillators with different combinations of geometric nonlinear stiffness terms*.

White Rose Research Online URL for this paper:  
<https://eprints.whiterose.ac.uk/176634/>

Version: Published Version

---

**Article:**

Nasir, A., Sims, N. and Wagg, D. [orcid.org/0000-0002-7266-2105](https://orcid.org/0000-0002-7266-2105) (2021) Direct normal form analysis of oscillators with different combinations of geometric nonlinear stiffness terms. *Journal of Applied and Computational Mechanics*, 7 (Special Issue). pp. 1167-1182.

10.22055/JACM.2021.34016.2324

---

**Reuse**

This article is distributed under the terms of the Creative Commons Attribution-NonCommercial (CC BY-NC) licence. This licence allows you to remix, tweak, and build upon this work non-commercially, and any new works must also acknowledge the authors and be non-commercial. You don't have to license any derivative works on the same terms. More information and the full terms of the licence here:  
<https://creativecommons.org/licenses/>

**Takedown**

If you consider content in White Rose Research Online to be in breach of UK law, please notify us by emailing [eprints@whiterose.ac.uk](mailto:eprints@whiterose.ac.uk) including the URL of the record and the reason for the withdrawal request.



[eprints@whiterose.ac.uk](mailto:eprints@whiterose.ac.uk)  
<https://eprints.whiterose.ac.uk/>



# Journal of Applied and Computational Mechanics



Research Paper

## Direct Normal Form Analysis of Oscillators with Different Combinations of Geometric Nonlinear Stiffness Terms

Ayman Nasir<sup>✉</sup>, Neil Sims<sup>✉</sup>, David Wagg<sup>✉</sup>

Department of Mechanical Engineering, The University of Sheffield, Sheffield, S1 3JD, UK, Emails: amnasir1@sheffield.ac.uk, n.sims@sheffield.ac.uk, david.wagg@sheffield.ac.uk

Received June 26 2020; Revised May 26 2021; Accepted for publication May 27 2021.

Corresponding author: A. Nasir (amnasir1@sheffield.ac.uk)

© 2021 Published by Shahid Chamran University of Ahvaz

**Abstract.** Nonlinear oscillators with geometric stiffness terms can be used to model a range of structural elements such as cables, beams and plates. In particular, single-degree-of-freedom (SDOF) systems are commonly studied in the literature by means of different approximate analytical methods. In this work, an analytical study of nonlinear oscillators with different combinations of geometric polynomial stiffness nonlinearities is presented. To do this, the method of direct normal forms (DNF) is applied symbolically using Maple software. Closed form (approximate) expressions of the corresponding frequency-amplitude relationships (or backbone curves) are obtained for both  $\varepsilon$  and  $\varepsilon^2$  expansions, and a general pattern for  $\varepsilon$  truncation is presented in the case of odd nonlinear terms. This is extended to a system of two degrees-of-freedom, where linear and nonlinear cubic and quintic coupling terms exist. Considering the non-resonant case, an example is shown to demonstrate how the single mode backbone curves of the two degree-of-freedom system can be computed in an analogous manner to the approach used for the SDOF analysis. Numerical verifications are also presented using COCO numerical continuation toolbox in Matlab for the SDOF examples.

**Keywords:** Nonlinear, Mechanical Vibrations, Direct Normal Forms, Backbone curves, Symbolic computations.

### 1. Introduction

The analysis of single-degree-of-freedom (SDOF) nonlinear oscillators has been widely studied in the nonlinear dynamics literature, especially for oscillators that have just one geometric polynomial nonlinear stiffness term. Due to the historic development of the topic, and the richness of the dynamics exhibited by these oscillators many studies have focused on quadratic and cubic nonlinearities, while higher order nonlinearities are much less widely studied. That said, there have been a number of studies where the analysis is extended to involve two combinations of different nonlinear stiffness terms, typically limited to low polynomial orders - see for example [4,5,7,12,13,16,19] and references therein.

In this paper, nonlinear oscillators with different combinations of geometric nonlinear stiffness terms are studied using the direct normal form (DNF) method developed by Neild and Wagg [14], and used to obtain approximate analytical solutions for the (conservative) backbone curves (e.g. frequency-amplitude curves) of both SDOF and a two-degree-of-freedom nonlinear system. One objective of this is to consider the larger amplitude response of these types of oscillators, for which higher order terms become significant.

The DNF method is an approximate method for analyzing weakly nonlinear systems with typically smooth nonlinearities. Like other normal form methods, it is based on the development of a linear homological equation which enables resonant and non-resonant cases to be analyzed. Once the homological equation has been solved to provide a nonlinear near-identity normal form transformation, approximate analytical frequency-amplitude relationships, otherwise known as conservative backbone curves can be obtained. The relationship between the DNF and a selection of other approximate mathematical methods is discussed in Alexander et al. [8].

The step-by-step nature of the direct normal form method means that it can readily be implemented using symbolic computation techniques. This approach can help mitigate the algebraic complexity that tends to occur as more nonlinear terms, and/or degrees-of-freedom are added. The main focus here is to use symbolic computation software (Maple in this case), to study higher order geometric nonlinear terms that appear in the equations of motion in the form of polynomial stiffness terms, in the literature, Maple has been used in the field of nonlinear dynamics in a number of conducted works, for instance, refer to [2,20,21]. The traditional analysis of the DNF method depends on hand manipulations to generate the desired backbone curve relations, and then numerical or experimental verifications are performed in order to validate the analytical results. Despite being effective in some relatively simple cases, this traditional method becomes increasingly difficult, if not impossible, as the complexity increases, such as the case when higher orders of nonlinear terms are added to the equations of motion.

In the field of nonlinear dynamics, the DNF technique has been used to conduct a number of research works. For instance, Xin et al. [1], studied SDOF nonlinear oscillators of polynomial-type nonlinearities. In their work, an extensive study of velocities and displacements associated with nonlinear system is presented, and the resulting resonance response functions (RRFs) were used for illustrating the contributions of the several polynomial nonlinearities appearing in the system. Another related work was conducted



by Shaw et al. [4], in which the authors explored the performance of nonlinear vibration isolators using the DNF method. The system was modelled by a SDOF oscillator and estimations of a group of conservative backbone curves were obtained.

In the wider literature, the analysis of SDOF nonlinear oscillators with high orders of geometric polynomial nonlinearities is restricted to a few cases where the application of approximate analytical methods is achievable. In respect to the order of the nonlinear terms, one of the most complicated systems studied is the cubic-quintic oscillator. This type of oscillator was studied in detail by Nayfeh using the method of renormalization (RN or uniformization), [16], where an approximate backbone curve relation under the assumption of small amplitudes is obtained. Another study of the cubic-quintic oscillator using approximate techniques was carried out Suleman and Wu [6]. Here the authors introduced a set of backbone curves of such an oscillator based on the condition of small amplitudes of vibrations, and then used several methods for the analysis including an energy balance method (EBM), the modified homotopy perturbation method (modified HPM) and the global error minimization method. The results were compared to show that the modified HPM method leads to the most accurate results for that study. In this work, for verification purposes, the generated results for nonlinear cubic-quintic conservative oscillator using DNF are compared to the results of Nayfeh (RN method) and the Homotopy method. All of these results are also compared with numerical results generated using a Runge-Kutta method.

In the literature, some other combined methods of solution, mostly perturbation based, are found; for instance, Razzak [7] used a combined technique of homotopy perturbation along with variational formulation to obtain approximations for the nonlinear frequency of the cubic-quintic oscillator and this method yields accurate results for both weak and strong nonlinearities. However, in different homotopy methods, the trial solutions are arbitrarily chosen such that the resulting solution converges to acceptable levels of accuracy, and as a result the trial solution needs to be adjusted in terms of the type and order of the nonlinear terms. One of the advantages of the DNF technique is the consistency of the solution, and the generality of the assumed solution; the consecutive steps of the solution lead to the possibility of investigating various systems regardless of the trial solution shape and accuracy.

In order to generalize the applications of DNF method for SDOF nonlinear oscillators with a different number and/or order of polynomial stiffness nonlinear terms, a system containing four types of nonlinearities, including both odd and even orders, is studied in detail, and backbone curves of both  $\varepsilon$  and  $\varepsilon^2$  accuracies are generated. This is followed by a general closed-form expression of  $\varepsilon$  accuracy, and a discussion of the effectiveness of extending the analysis to higher order accuracies.

In the final part of the paper, an analysis of a two degree-of-freedom system is presented. In this example, the methodology presented for SDOF systems is extended to two degrees-of-freedom, and for the non-resonant case, expressions for backbone curves are obtained. This example helps to demonstrate how the analysis can potentially be extended to other multi-degree-of-freedom systems that include higher order polynomial nonlinear terms.

## 2. Methodology

The direct normal forms technique involves the application of linear and nonlinear transformations (or near-identity transformations) to the equation of motion, in order to identify the resonant terms and get approximate analytical solutions for the system. The complete analysis of this method is discussed in detail in [14], in this Section, a summary of the essential steps is shown. For the case of undamped, unforced vibrating systems, the technique is applied using four main consecutive steps:

Step 1: Decoupling linear terms using linear modal transformation.

Step 2: Derivation of the homological equation for the nonlinear near-identity transformation.

Step 3: Applying the near-identity transformation to the transformed equation of motion from Step 2.

Step 4: Finally, solving the resulting normal forms equation (or set of equations) to obtain backbone curve relationships.

Moreover, systems that are externally forced require an additional transformation, due to the presence of the forcing term. The forcing transformation involves the removal of any non-resonant forcing terms. In practice, viscous damping is usually included in with the nonlinear terms (see [14] for details). A more detailed mathematical description of the DNF for analyzing conservative SDOF systems is given in Appendix 1, while the analysis of higher orders accuracy is shown in Appendix 2.

## 3. Analysis of cubic-quintic SDOF oscillator

In this Section, the analysis of different types of nonlinear oscillators is briefly discussed. The first example illustrates the conservative (undamped and unforced) cubic-quintic oscillator, which has been previously studied by a range of other researchers and so the results of DNF can be compared to their work. For instance, in ref. [10], Lai et al. have implemented a Newton-harmonic balancing approach to obtain first, second, and third-order approximations to the frequency-amplitude relationship for this type of SDOF oscillators. The interested reader can also find some other related works that study this system, see for example [6, 7 and 16].

The conservative cubic-quintic oscillator, as shown schematically in Fig. 1(a), is governed by the following equation of motion

$$m\ddot{x}(t) + kx(t) + \kappa_3 x^3(t) + \kappa_5 x^5(t) = 0 \Rightarrow \ddot{x}(t) + \omega_n^2 x(t) + \varepsilon \alpha_1 x^3(t) + \varepsilon \alpha_2 x^5(t) = 0, \quad (1)$$

where an over dot represents the derivative with respect to time,  $x$  represents the physical displacement,  $m$  is the mass of the oscillator, and the linear, cubic and quintic stiffnesses are  $k$ ,  $\kappa_3$  and  $\kappa_5$ , respectively, the subscripts are chosen to reflect the order of the nonlinearity (this can be helpful when studying multi-degree-of-freedom systems, as will be discussed in Section 5). Moreover,  $\omega_n$  is the natural frequency of the system,  $\varepsilon \alpha_1$  and  $\varepsilon \alpha_2$  are (assumed to be small) coefficients for the cubic and quintic nonlinear terms, respectively, in this work we use  $\varepsilon$  as a bookkeeping parameter (assumed to be unity here and will appear during the analysis of the DNF method to denote the level of accuracy). Firstly, by applying the linear modal transformation, the transformation is unity so  $x = q$ , and this is applicable for any SDOF system, then

$$\ddot{q} + \Lambda q + N_q(q) = 0, \quad (2)$$

where  $\Lambda = \omega_n^2$  and  $N_q(q) = \alpha_1 q^3 + \alpha_2 q^5$ . The second step is the near-identity transformation, and for  $\varepsilon$  accuracy, rewriting the nonlinear terms using  $u$ , in view of Eq. (A.12) in Appendix 1, one should obtain  $N_q(u) = \alpha_1 u_1^3 + \alpha_2 u_1^5$ , thus

$$n_{(1)}(u) = \mathbf{n}^* \mathbf{u}^*(u_p, u_m) = \alpha_1 (u_p + u_m)^3 + \alpha_2 (u_p + u_m)^5 \quad (3)$$

By expanding Eq. (3),  $n_{(1)}(u)$  will contain many terms (ten terms in this case), these terms have to be primarily decomposed into coefficients and nonlinear functions vectors  $\mathbf{n}^*$  and  $\mathbf{u}^*$ , respectively. For this example



$$\mathbf{n}^* = [\alpha_1 \quad \alpha_2 \quad \alpha_1 \quad \alpha_2 \quad 3\alpha_1 \quad 5\alpha_2 \quad 3\alpha_1 \quad 10\alpha_2 \quad 10\alpha_2 \quad 5\alpha_2] \tag{4a}$$

$$\mathbf{u}^* = [u_m^3 \quad u_m^5 \quad u_p^3 \quad u_p^5 \quad u_p u_m^2 \quad u_p u_m^4 \quad u_p^2 u_m \quad u_p^2 u_m^3 \quad u_p^3 u_m^2 \quad u_p^4 u_m]^T \tag{4b}$$

The crucial step in this solution is solving the homological equation by finding the  $\beta^*$  matrix (refer to Eqs. (A.14) and (A.15) in Appendix 1). To proceed, the polynomial term indices (defined by  $s_p$  and  $s_m$ ) in the vector  $\mathbf{u}^*$  need to be found.

In the present study, the above analysis has been implemented symbolically, and in principle this approach can be extended to any finite number of terms in Eq. (4). The next step defines the transformed nonlinear terms ( $\mathbf{n}_{u,l}^*$ ) and harmonics ( $\mathbf{h}_i^*$ ) matrices, (refer to Eq. (A.16) in Appendix 1). In practice, in Maple, this is performed by applying several iterative loops for each element in  $\beta^*$ . For this example system, Table 1 shows all the terms in Eq. (4b) and the corresponding  $s_p$ ,  $s_m$  and  $\beta^*$ . It is noteworthy to mention that traditional hand calculations are performed by generating matrices (or tables) similar to Table 1, which quickly becomes impractical for more complex systems, on the other hand, the proposed symbolic computation method automatically generates all of these matrices, thus eliminates the chance of any mathematical errors, reduces the time and effort of computation and enables the study of more complex systems (within the constraint of the available computing power).

If the truncated solution is limited to  $\varepsilon$  order, the final step is rewriting the transformed equation of motion. For the non-resonant terms to  $\varepsilon$  accuracy, the equation of motion in the  $u$ -transformed coordinate system becomes

$$\ddot{u} + \Lambda u + \mathbf{n}_u^* \mathbf{u}^* = 0, \tag{5}$$

which can be written as

$$\ddot{u} + \omega_n^2 u + 3\alpha_1(u_p u_m^2 + u_p^2 u_m) + 10\alpha_2(u_p^2 u_m^3 + u_p^3 u_m^2) = 0, \tag{6}$$

and the near identity transformation is written as

$$q = u + \mathbf{h}^* \mathbf{u}^*, \tag{7}$$

which leads to

$$q = u + \frac{1}{8\omega_r^2} \left( \alpha_1(u_p^3 + u_m^3) + \frac{\alpha_2}{3}(u_p^5 + u_m^5) + 5\alpha_2(u_p^4 u_m + u_p u_m^4) \right) \tag{8}$$

In order to generate a time domain solution of the system, one can easily substitute the assumed solution, (Eq. (A.12) in Appendix 1) in Eq. (8). Nevertheless, the focus in this work is to study the frequency amplitude relationship for the conservative (i.e. undamped) system, or the so-called conservative backbone curve. This can be also obtained by substituting in the assumed solution and solving the positive (or negative) complex exponential terms using exact harmonic balancing. Finally, using this approach the backbone curve, truncated to  $\varepsilon$  accuracy, is expressed as

$$\omega_r^2 = \omega_n^2 + \frac{3}{4}\alpha_1 U^2 + \frac{5}{8}\alpha_2 U^4 \tag{9}$$

This form of  $\varepsilon$  order backbone curve will be adopted for analyzing the nonlinear frequency of the cubic-quintic oscillator, however, the results of Eq. (9) will also be compared to  $\varepsilon^2$  solution, as will be discussed in the next Section.

### 3.1 Higher order accuracy

A direct normal form analysis of  $\varepsilon^2$  expansion for the same cubic-quintic oscillator is to be discussed in this section. The solution is based on the results of  $\varepsilon$  accuracy, hence, it is possible to write

**Table 1.** DNF matrix results for the cubic-quintic oscillator computed to  $\varepsilon$  accuracy, if  $\beta_i^* = 0$ , a resonance is indicated, otherwise the term is considered to be a non-resonant term.

$\mathbf{u}_i^*$	$s_p$	$s_m$	$\beta_i^*$	$\mathbf{n}_{u,l}^*$	$\mathbf{h}_i^*$
$u_m^3$	0	3	$8\omega_r^2$	0	$\frac{\alpha_1}{8\omega_r^2}$
$u_m^5$	0	5	$24\omega_r^2$	0	$\frac{\alpha_2}{24\omega_r^2}$
$u_p^3$	3	0	$8\omega_r^2$	0	$\frac{\alpha_1}{8\omega_r^2}$
$u_p^5$	5	0	$24\omega_r^2$	0	$\frac{\alpha_2}{24\omega_r^2}$
$u_p u_m^2$	1	2	0	$3\alpha_1$	0
$u_p u_m^4$	1	4	$8\omega_r^2$	0	$\frac{5\alpha_2}{8\omega_r^2}$
$u_p^2 u_m$	2	1	0	$3\alpha_1$	0
$u_p^2 u_m^3$	2	3	0	$10\alpha_2$	0
$u_p^3 u_m^2$	3	2	0	$10\alpha_2$	0
$u_p^4 u_m$	4	1	$8\omega_r^2$	0	$\frac{5\alpha_2}{8\omega_r^2}$



$$u_u = \mathbf{n}_u^* \mathbf{u}^* = 3\alpha_1(u_p u_m^2 + u_p^2 u_m) + 10\alpha_2(u_p^2 u_m^3 + u_p^3 u_m^2) \tag{10}$$

$$\mathbf{h}^* \mathbf{u}^* = \frac{1}{8\omega_r^2} \left( \alpha_1(u_p^3 + u_m^3) + \frac{\alpha_2}{3}(u_p^5 + u_m^5) + 5\alpha_2(u_p^4 u_m + u_p u_m^4) \right)$$

moreover,  $n_1(u) = \alpha_1 u^3 + \alpha_2 u^5$  and its Jacobian is  $\frac{d}{du}\{n_1(u)\} = 3\alpha_1 u^2 + 5\alpha_2 u^4$ . Now, the pre-transformed nonlinear term,  $\tilde{n}_2$ , is given by

$$\tilde{n}_2(u) = \frac{1}{4\omega_r^2} \left( \frac{\alpha_1}{4} + \frac{\alpha_2}{12} + \frac{5\alpha_2}{4} \right) (\omega_n^2 - \omega_r^2) + (3\alpha_1 u^2 + 5\alpha_2 u^4) \tag{11}$$

Herein, it is important to notice that no  $\varepsilon^2$  related terms appear in the original EOM, and so  $\mathbf{n}_2 = 0$ . To complete the analysis, Eq. (11) needs to be expanded and the same previous procedure is repeated, with more terms appearing in the expansion compared to  $\varepsilon$  accuracy (26 terms compared to 10 terms), due to the large number of terms, only the key results are to be shown here, detailed results are shown in Table A1 (Appendix 3). The equation of motion in the  $u$ -transformed coordinate system becomes

$$\ddot{u} + \Lambda u + \mathbf{n}_u^* \mathbf{u}^* + \mathbf{n}_u^+ \mathbf{u}^+ = 0, \tag{12}$$

$$\ddot{u} + \omega_n^2 u + 3\alpha_1(u_p u_m^2 + u_p^2 u_m) + 10\alpha_2(u_p^2 u_m^3 + u_p^3 u_m^2) = 0,$$

and the near identity transformation is written as

$$q = u + \mathbf{h}^* \mathbf{u}^* + \mathbf{h}^+ \mathbf{u}^+, \tag{13}$$

which leads to

$$q = u + \frac{1}{8\omega_r^2} \left( \alpha_1(u_p^3 + u_m^3) + \frac{\alpha_2}{3}(u_p^5 + u_m^5) + 5\alpha_2(u_p^4 u_m + u_p u_m^4) \right) \tag{14}$$

The conservative backbone curve, truncated to  $\varepsilon^2$ , can be obtained by substituting in the assumed solution Eq. (14), and solving the positive (or negative) complex exponential terms using exact balancing, primarily, we get the following form

$$\omega_r^2 = \omega_n^2 + \frac{3}{4}\alpha_1 U^2 + \frac{5}{8}\alpha_2 U^4 + \frac{3}{128\omega_r^2}\alpha_1^2 U^4 + \frac{5}{64\omega_r^2}\alpha_1\alpha_2 U^6 + \frac{95}{1536\omega_r^2}\alpha_2^2 U^8 \tag{15}$$

In Eq. (15), the effect of  $\varepsilon^2$  can be interpreted as a type of frequency correction parameter. While most of the researchers using direct normal forms are only considering  $\varepsilon$  accuracy in the solution, it has previously been noticed that in some cases extending the analyses to include  $\varepsilon^2$  accuracy can effectively enhance the results - refer to [11] as an example. In order to verify the accuracy of the solution, we will compare both  $\varepsilon$  and  $\varepsilon^2$  solutions with the numerical solution obtained using a 4<sup>th</sup> order Runge-Kutta computation in Matlab, and sample results are shown in Fig. (1). In Fig. (1)(b-c), both steady state response of the oscillator and phase portrait plots are shown for  $\varepsilon$  and  $\varepsilon^2$  along with the numerical solution. Overall, results in Fig. (1) show excellent agreement between the approximate DNF solutions and the numerical solution.

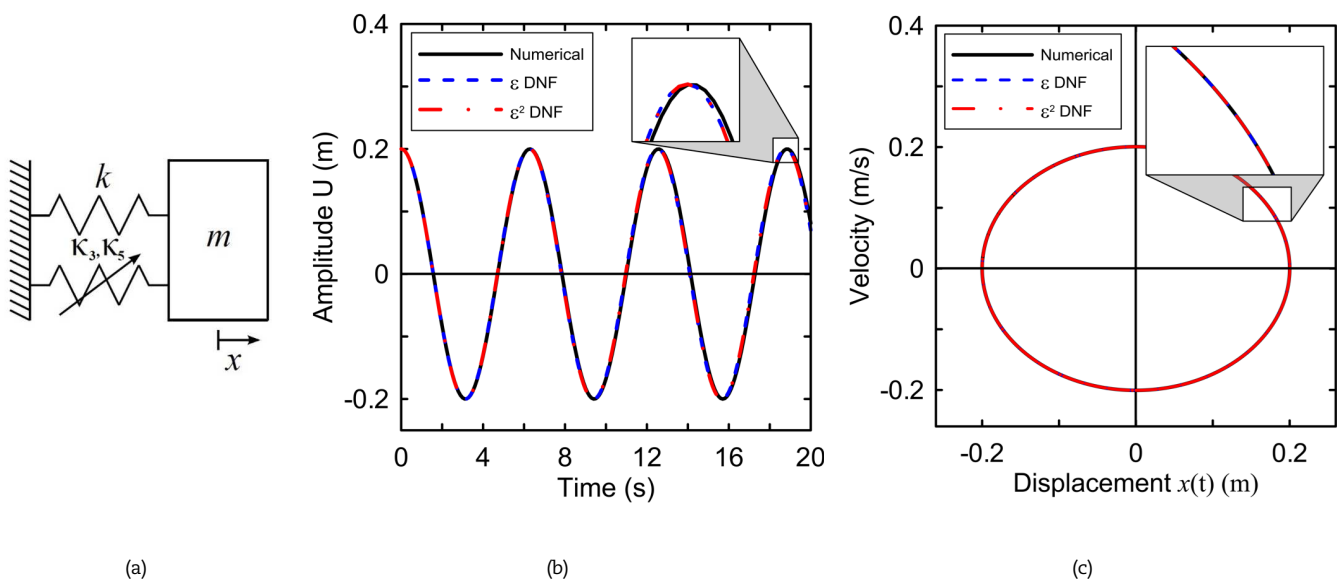


Fig. 1. DNF results compared to numerical results: (a) Schematic diagram of the cubic-quintic oscillator shown in Eq. (1), (b) Steady state response, (c) Phase portrait. The dashed blue curve and dash-dotted lines are computed from the analytical DNF solution for both  $\varepsilon$  and  $\varepsilon^2$ , respectively, while the solid black curves are the numerical solutions computed using 4<sup>th</sup> order Runge-Kutta computation in Matlab. Parameter values are:  $\omega_n = 1$  rad/s,  $\alpha_1 = \alpha_2 = 0.1$ .



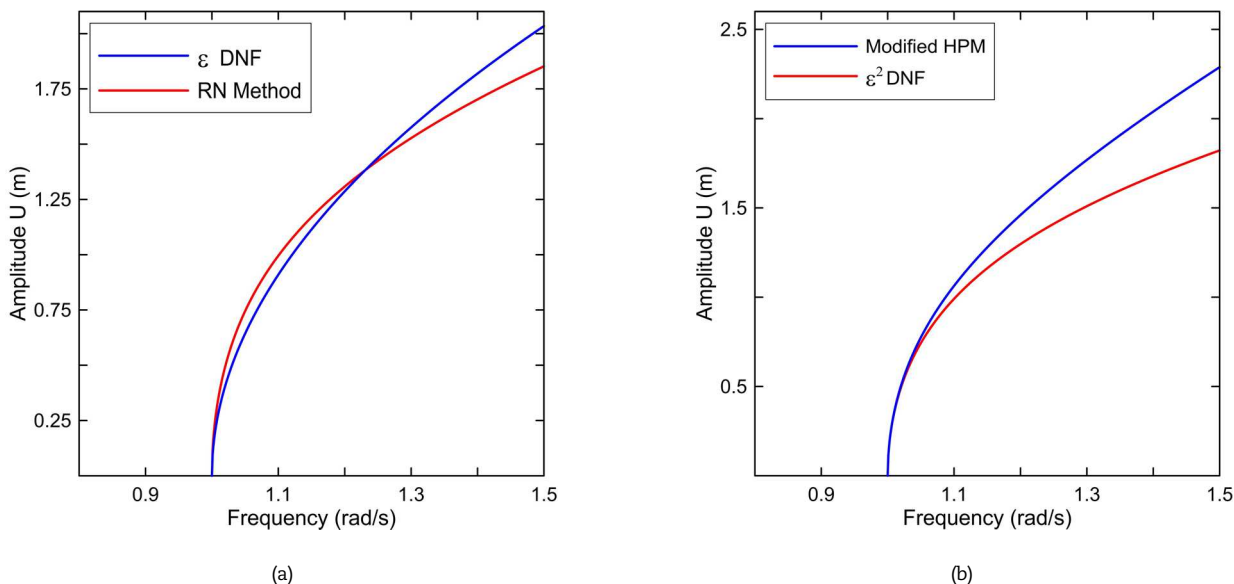


Fig. 2. Comparison between DNF results and other methods for the cubic-quintic oscillator: (a) ε-order DNF and the method of Renormalization (RN method), (b) ε²-order DNF and the modified homotopy method (Modified HPM). Parameter values are: ω<sub>n</sub> = 1 rad/s, α<sub>1</sub> = 0.2 and α<sub>2</sub> = 0.1.

3.2 Comparisons with other methods

In order to verify the results of both ε and ε² accuracies, it is possible to compare with some previous results in the literature. For ε accuracy, Nayfeh’s approximation for small amplitudes [16] has the following form

$$\omega_r = 1 + \left( \frac{3}{8} \alpha_1 + \frac{5}{16} \alpha_2 U^2 \right) U^2 \tag{16}$$

Hence, the ε DNF solution given by Eq. (9) can be compared to Eq. (16) for primary verification of the validity of the DNF solution. Eq. (16) is valid for small amplitudes; thus Fig. (2)(a) shows a comparison between both solutions for the following numerical values: α<sub>1</sub> = 0.2, α<sub>2</sub> = 0.1. This figure shows good agreement between the two approximations, specifically when the forcing frequency is close to the linear frequency, while at higher frequencies the two methods diverge.

Furthermore, in the literature, some researchers studied the cubic quintic oscillator to ε² accuracy. For instance, Suleman and Wu [6] used a modified homotopy method (modified HPM) to derive the backbone curve of this oscillator in the form

$$\omega_r = \sqrt{\frac{1}{2} \left( 1 + \frac{3}{4} \alpha_1 U^2 + \sqrt{\left( \left( 1 + \frac{3}{4} \alpha_1 U^2 \right)^2 + \frac{15}{4} \alpha_1^2 U^4 + \frac{35}{144} \alpha_2^2 U^4 \right)} \right)} \tag{17}$$

For verification purposes, the results of DNF for ε² accuracy, Eq. (15), can be compared to Eq. (17), in addition to the numerical solution of the cubic-quintic oscillator, as will be shown in Tables 2-4. However, as a primary comparison, Fig. (2)(b) shows a comparison between the approximated backbone curves from both techniques. The two curves in Fig. (2)(b) show identical behavior at low amplitude, but the curves diverge as amplitudes of vibration increase, particularly for amplitude values above one. Further details regarding the accuracy of the two solutions will be shown in the next Sections.

3.4 Numerical investigation of the frequency-amplitude relationship

In order to verify the results of the analytical approximate methods previously described, some numerical techniques can be used. Specifically, Runge-Kutta methods can be used to find the steady-state frequency response of Eq. (1) for any given parameter values, and compared with the results of RN, HPM and DNF (ε and ε²) in order to compare the accuracy of these methods. For numerical verification purposes, the numerical solution is generated using ODE45 in Matlab with step size of 10<sup>-6</sup>, additionally, the numerical results are compared with the elliptical function solution of Duffing oscillator which already exists in the literature.

Based on the Jacobi elliptic functions, the elliptical function solution (EPS) of Duffing oscillator has been studied by several authors, and the results are summarized by Kovacic and Brennan [22]. This work is to be adopted for validating the numerical solution. By setting α<sub>2</sub> = 0 in Eq. (1), we get the equation of the conservative Duffing oscillator, which is

$$\ddot{x}(t) + \omega_n^2 x(t) + \alpha_1 x^3(t) = 0 \tag{18}$$

According to Kovacic and Brennan [22], the nonlinear frequency of this oscillator is

$$\omega_r^2 = (\omega_n^2 + \alpha_1 U^2) \left( 1 - \frac{\alpha_1 U^2}{4 \omega_n^2} \left( 1 - \frac{\alpha_1 U^2}{4} \right) \right) + \dots \tag{19}$$

For verification purposes, the numerical solution used in this work is applied to the Duffing oscillator, Eq. (18) and the numerical results of the nonlinear frequency are compared to the results of Kovacic and Brennan [29]. Sample results of this comparison can be found in Fig. (3), in which both the EPS and the numerically obtained backbone curves are plotted for α<sub>1</sub> = 0.1. From this figure it can be seen that numerical solution has acceptable levels of accuracy at frequencies that are close to the natural frequency of the system while the accuracy decreases at higher values of the dimensionless nonlinear frequency.



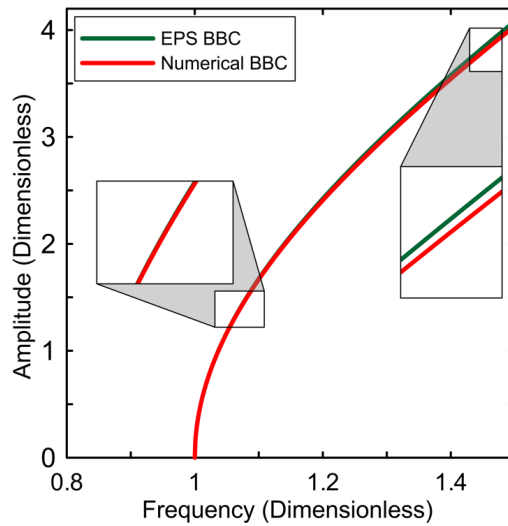


Fig. 3. Comparison between elliptical functions (EPS) and numerical backbone curves for the Duffing oscillator. Parameter values used are:  $\omega_n = 1$  rad/s and  $\alpha_1 = 0.2$ .

### 3.5 Comparing analytical results with numerical results for the cubic-quintic oscillator

Tables 2-3 show comparisons between Nayfeh’s results (denoted by RN method), Suleman and Wu results (denoted by Modified HPM) and the proposed method using DNF for both  $\varepsilon$  and  $\varepsilon^2$ , all compared to the numerical Runge-Kutta results (as a reference for comparison). The comparison is carried out for different selected amplitude values in order to evaluate the nonlinear amplitude-frequency response of the system while the linear natural frequency is assumed to be unity in all cases. Absolute error relative to the numerical solution is also shown as a percentage underneath each of the relevant entries in the Table. In Table 2, the values selected for comparison are  $\alpha_1 = 0.2$  and  $\alpha_2 = 0.1$  in order to represent weak nonlinear terms in comparison to the linear term. While in Table 3, the effect of larger nonlinear terms is shown using the numerical values of  $\alpha_1 = 1$  and  $\alpha_2 = 1$ .

The results in Tables 2-3 show the accuracy of direct normal forms method compared to some other well established approximate methods that already exist in the literature. It is clear that, in terms of accuracy, the DNF method gives acceptable approximation of the frequency shift due to the presence of nonlinear terms in the equations of motion. The DNF method has been classified into two approaches  $\varepsilon$  and  $\varepsilon^2$ , and in terms of the series expansion, and this should correlate to lower and higher accuracies, respectively. However, the higher order accuracy does not always show a reduction in error compared to the  $\varepsilon$  approach. A potential reason for this is due to the fact that only odd nonlinear terms are present, further explanation of this point is given in Section 4.

From another point of view, in order to explore the effect of changing the nonlinear coefficients,  $\alpha_1$  and  $\alpha_2$ , on the nonlinear frequency of the system, it is possible to make a parametric study of the resulting backbone curve equations. For instance, using the amplitude of  $U= 0.2$ , the nonlinear frequency of the system, truncated to  $\varepsilon$  accuracy, can be computed when the nonlinear coefficients are changing steadily from -1.0 to 1.0, results of this sample study are found in Table 4.

Table 2. DNF method results compared with other methods for  $\alpha_1 = 0.2, \alpha_2 = 0.1$ , the natural frequency chosen is  $\omega_n = 1$  rad/s

Amplitude $U$	Numerical	RN method	Modified HPM	$\varepsilon$ DNF	$\varepsilon^2$ DNF
0.05	1.000283	1.000188	1.000188	1.000187	1.000187
		0.002 %	0.009 %	0.009 %	0.009 %
0.2	1.003119	1.003050	1.003026	1.003045	1.003045
		0.171 %	0.009 %	0.007 %	0.007 %
0.5	1.020481	1.020703	1.019777	1.020493	1.020543
		0.022 %	0.491 %	0.421 %	0.416 %
1.0	1.104164	1.106250	1.090601	1.101136	1.101986
		0.189 %	1.228 %	0.274 %	0.197 %
2.0	1.595567	1.800000	1.509942	1.612451	1.633491
		12.813 %	5.366 %	1.058 %	2.377 %
5.0	6.098712	22.406250	5.916005	6.619101	6.979045
		267.39 %	2.996 %	8.533 %	14.435 %

Table 3. DNF method results compared with other methods for  $\alpha_1 = 1, \alpha_2 = 1$ , the natural frequency chosen is  $\omega_n = 1$  rad/s

Amplitude $U$	Numerical	RN method	Modified HPM	$\varepsilon$ DNF	$\varepsilon^2$ DNF
0.05	1.001028	1.000939	1.000938	1.000939	1.000939
		0.009 %	0.009 %	0.009 %	0.009 %
0.2	1.015361	1.015500	1.015216	1.015382	1.015414
		0.014 %	0.0142 %	0.0020 %	0.0052 %
0.5	1.106532	1.113281	1.101490	1.107503	1.108546
		0.610 %	0.4556 %	0.0877 %	0.1820 %
1.0	1.523596	1.687500	1.473823	1.554790	1.541104
		10.758 %	3.2668 %	2.0474 %	1.1491 %
2.0	3.593537	7.500000	3.379416	3.741657	3.882786
		108.70 %	5.9585 %	4.1218 %	8.0491 %
5.0	19.18152	205.6875	18.07842	20.25772	21.49016
		972.32 %	5.751 %	5.611 %	12.036 %



**Table 4.** DNF method results for various values of the nonlinear coefficients, the natural frequency chosen is  $\omega_n = 1$  rad/s

Nonlinear Coefficients		Frequency $\omega_r$ (computed to $\varepsilon$ accuracy)				
$\downarrow \alpha_2$	$\rightarrow \alpha_1$	-1.0	-0.5	0.0	0.5	1.0
-1.0		0.984378	0.984653	0.984886	0.985140	0.985393
-0.5		0.991968	0.992225	0.992472	0.992724	0.992975
0.0		0.999500	0.999750	1.000000	1.000250	1.000500
0.5		1.006976	1.007224	1.007472	1.007720	1.007968
1.0		1.014412	1.014643	1.014889	1.015135	1.015402

To conclude, the results of cubic-quintic nonlinear oscillator with different values of the nonlinear coefficients has been implemented to study selected cases of oscillators in both hardening and softening cases. In addition, the approximate analytical results of DNF have been verified using numerical continuation techniques such as the COCO toolbox in Matlab [17,18]. COCO is used to numerically compute the frequency response functions representing the locus of points joining the maximum amplitude per period of the forced damped systems by adding viscous damping and periodic forcing terms to the cubic-quintic oscillator described in Eq. (1). Accordingly, using small damping value,  $\zeta = 0.01$ , Fig. (4) is generated for combinations of the nonlinear coefficients in the original equations of motion. In this figure, results for the linear oscillator, Duffing oscillator in both hardening and softening cases and the cubic-quintic oscillator in both hardening and softening cases are shown. The forced frequency response functions (dashed colored lines) are numerically computed using COCO, while the backbone curves (solid-colored lines) are computed using  $\varepsilon$  DNF results, Eq. (9). In Fig. (4), the idea is that the backbone curve should align along the center of the resonance curve (e.g. the COCO curve). The only point that the COCO and backbone should cross is near the peak of the resonance (COCO) curve. In Fig. (4), it can be seen that this is true, for all the cases considered. So, in this sense, the matching is good.

### 4. Analysis of generic cubic-quintic SDOF oscillator

In the previous Section, the results of  $\varepsilon$  DNF were shown to be accurate enough for the analyst to adopt, without the need to consider higher order terms, this is due the presence of odd nonlinear terms only in the original EOM. On the other hand, the presence of even nonlinear terms can raise the difficulty of the analysis. In this section, the system considered represents a more complicated case in which the oscillator has four different orders of polynomial nonlinear terms, in this example the effect of higher order accuracy,  $\varepsilon^2$ , can be explored. Finally, a general closed form relation of the backbone curve, truncated to  $\varepsilon$  accuracy is obtained for any oscillator with N number of stiffness polynomial nonlinear terms. In principle, Wagg and Neild [14] showed that, for the quadratic nonlinear oscillator,  $\varepsilon$  DNF will not be able to capture the nonlinear frequency-amplitude curve of the system, while extending the analysis to  $\varepsilon^2$  leads to a satisfactory approximation. In this section, using a SDOF oscillator with both odd and even nonlinear terms it is shown that the presence of even nonlinearities makes it necessary to compute  $\varepsilon^2$ .

Considering a SDOF nonlinear oscillator with four different orders of polynomial geometric nonlinear terms (with orders two to five, respectively), in its conservative form. The equations of motion of this oscillator can be written as

$$\ddot{x}(t) + \omega_n^2 x(t) + \alpha_1 x^2(t) + \alpha_2 x^3(t) + \alpha_3 x^4(t) + \alpha_4 x^5(t) = 0, \tag{20}$$

where the nonlinear coefficients are all assumed to be relatively small when compared to the linear term. Using the DNF, the objective is to find the backbone curves of this system. In such unforced systems, the analysis will be similar to that in the previous cubic-quintic system, with more terms to be computed (or correspondingly larger matrix sizes). For a DNF computed to  $\varepsilon$  accuracy, to find the number of terms, we can consider the following

- any nonlinear power  $\gamma$  will contribute by  $\gamma + 1$  terms, and this is accumulative according to the number of nonlinear terms in the EOM. Hence, the analysis of the oscillator in Eq. (23) involves 18 terms to be computed in the  $\varepsilon$  order solution.
- a viscous damping term, if appears in the equation of motion, will result in two additional terms, hence, the damped cubic-quintic oscillator involves 12 terms in that case.
- for the case of forced systems, more terms are to be included in the analysis according to the forcing type; either resonant or non-resonant. However, the analysis of this work is restricted to unforced, and non-resonant cases only.

Accordingly, the  $\varepsilon$  solution of the conservative oscillator in Eq. (23) results in 18 terms in the matrices, this number of terms is difficult to be manipulated by hand calculations, and this can justify turning to symbolic computations, moreover, the number of terms will also increase dramatically if considering  $\varepsilon^2$  solution, in fact the number of terms involved in  $\varepsilon^2$  analysis of Eq. (23) will be 52 terms.

Practically, DNF analysis of Eq. (20) will be similar to the cubic-quintic oscillator, with more terms to be included in the solution. Accordingly, only final results are shown in this section. The backbone curve, truncated to  $\varepsilon$  is found to be

$$\omega_r^2 = \omega_n^2 + \frac{3}{4} \alpha_1 U^2 + \frac{5}{8} \alpha_2 U^4 \tag{21}$$

which is identical to the equation obtained for the cubic-quintic oscillator, thus, it is clear that the effect of the even nonlinear terms in the original EOM is not appearing in the  $\varepsilon$  order results. If the analysis is extended to  $\varepsilon^2$ , the resulting backbone curve will be

$$\omega_r^2 = \omega_n^2 + \frac{3}{4} \alpha_1 U^2 + \frac{5}{8} \alpha_2 U^4 + \frac{1}{\omega_f^2} \left( \frac{3}{128} \alpha_2^2 U^4 + \frac{5}{64} \alpha_2 \alpha_4 U^6 + \frac{95}{1536} \alpha_4^2 U^8 - \frac{5}{6} \alpha_1^2 U^2 - \frac{7}{4} \alpha_1 \alpha_3 U^4 - \frac{63}{80} \alpha_3^2 U^6 \right) \tag{22}$$

Table 5 shows a comparison between  $\varepsilon$  and  $\varepsilon^2$  frequency results of this oscillator and the numerical results obtained using ODE45 in Matlab. For nondimensionalization purposes, similar to the cubic-quintic oscillator, the nondimensional numerical data chosen for Table 5 are  $\alpha_1 = \alpha_2 = \alpha_3 = \alpha_4 = 0.1$ . The results in Table 5 clearly show that the solutions truncated to  $\varepsilon^2$  are more accurate than those truncated a  $\varepsilon$ , which is a consequence of the presence of even nonlinear terms in the original equations of motion. For this particular system, the accuracy of the approximate analytical results is slightly modified due to calculating the higher order expansion. Nevertheless, in some other cases it can be necessary to find  $\varepsilon^2$  solution; for example, if only even nonlinear terms appear in the equation of motion.





**Table 5.** DNF results for various values of the nonlinear coefficients, the natural frequency chosen is  $\omega_n = 1$  rad/s and  $\alpha_1 = \alpha_2 = \alpha_3 = \alpha_4 = 0.1$ .

$U$	Numerical	$\epsilon$	$\epsilon^2$
0.05	1.00018	1.00009 0.008 %	1.00014 0.005 %
0.1	1.00043	1.00033 0.010 %	1.00035 0.008 %
0.2	1.00147	1.00155 0.007 %	1.00137 0.011 %
0.5	1.01017	1.01126 0.108 %	1.00967 0.049 %
1	1.06428	1.06653 1.21 %	1.05288 0.869 %
2	1.45567	1.51657 1.52 %	1.47312 1.25 %
3	2.75600	2.59567 2.51 %	2.61570 1.86 %
4	3.83312	4.86614 3.21 %	4.30962 2.10 %
5	6.5698	6.27592 4.47 %	6.65439 2.45 %

It has been shown that the analysis of a nonlinear oscillator with a single quadratic nonlinearity (the escape equation) using DNF truncated to  $\epsilon$  accuracy (refer to [14] for more details) is not sufficient to compute the backbone curve relation, in fact the  $\epsilon^2$  order analysis is required.

In this work, it is shown that this result is true for higher order even nonlinear terms, and Table A2 (in Appendix 4) summarizes the results of the backbone curves for both lower and higher accuracies computed up to the 15<sup>th</sup> polynomial order of the nonlinear terms. For verification purposes of the approximate analytical results of DNF, it is possible to compare with numerical continuation (COCO). Hence, Fig. (5) shows a comparison between DNF truncated to both  $\epsilon$  and  $\epsilon^2$ , along with the numerical solution of the related forced damped system. The numerical data are  $\alpha_1 = \alpha_2 = \alpha_3 = \alpha_4 = 0.1$ .

Using Fig. (5), it is clear that good matching between DNF results and the numerical results, in terms of the backbone curve curvature being very close to the center line of the COCO computed curve. However, the backbone curves are not intersecting exactly at the peak of the COCO curve. One reason for this is related to the damping ratio used for computing the numerical results. The COCO simulations include a viscous damping term, which was chosen to be  $\zeta = 0.01$  in this case, while the backbone curves are computed for conservative systems. If damped backbone curves were computed, better matching between the backbones and COCO curves would be expected.

**4.1 Analysis of SDOF oscillators with any type of odd polynomial nonlinearities**

The equation of motion for a general SDOF conservative oscillator, with multiple geometric (polynomial) odd nonlinearities can be written as

$$\ddot{x}(t) + \omega_n^2 x(t) + N_x = 0, \tag{23}$$

where  $\omega_n$  is the natural frequency and the nonlinear terms vector  $N_x$ , in its general form, is written as

$$N_x = \sum_{i=1}^R \alpha_i x^i(t) \tag{24}$$

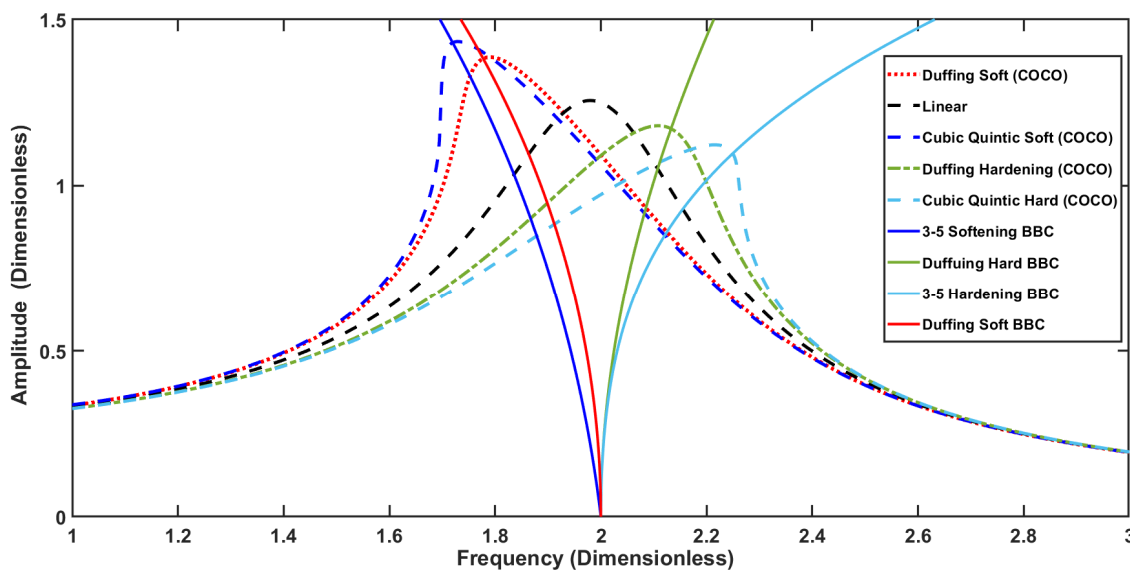


**Fig. 4.** Backbone curves and forced frequency response functions for different values of the nonlinear coefficients; solid lines represent backbone curves and dashed lines show the locus of the maximum displacement amplitude of the equivalent period orbit with forcing and damping added. Parameter values are:  $\omega_n = 2$  rad/s, and  $\alpha_1 = \alpha_2 = 0.1$  for the hardening cases, and  $\alpha_1 = \alpha_2 = -0.1$  for the softening cases.



**Table 6.** Values of the constants  $\xi_j$  for  $\varepsilon$  order DNF

Order of nonlinearity	3	5	7	9
$\xi_j$	$\frac{3}{4}$	$\frac{5}{8}$	$\frac{35}{64}$	$\frac{63}{128}$

Herein,  $\alpha_i$ , the coefficient of the  $i$ -th nonlinear stiffness term is considered to be relatively small, and  $R$  denotes the number of odd nonlinear terms. Using the method of DNF (implemented symbolically), the corresponding backbone curves of Eq. (23) have been generated. It was found that, for  $\varepsilon$  order only, the effect of any odd nonlinearity appearing in the equation of motion is additive in the resulting expression for the backbone curve. For instance, the  $\varepsilon$  order solution of the cubic-quintic oscillator will contain the terms of the cubic oscillator plus a term from the quintic oscillator. As a result, the corresponding expression for the backbone curve truncated to  $\varepsilon$  order can be written as

$$\omega_r^2 = \omega_n^2 + \sum_{j=1}^R \xi_j \alpha_j U^{2j+1} \quad (25)$$

where  $\xi_j$  are constant coefficients appearing in the backbone curve equation, (these coefficients are independent of the nonlinear coefficients, or  $\alpha$  values appearing in the original equation of motion). Table 6 shows the leading values of these constant coefficients for the first four orders of odd nonlinearities.

Thus, using Eq. (25) and the values from Table 6, DNF results truncated to  $\varepsilon$  accuracy, for the conservative backbone curve can be obtained. However, by using the binomial coefficients it can be shown that for any odd order  $j$  the coefficients  $\xi_j$  are given by the general expression

$$\xi_j = \frac{1}{2^{j-1}} \binom{j}{\frac{j+1}{2}}, \quad j = 1, 3, 5, \dots \quad (26)$$

Hence, the backbone curve equation, truncated to  $\varepsilon$  order, for a SDOF oscillator with odd polynomial nonlinear stiffness terms, can be written as

$$\omega_r^2 = \omega_n^2 + \sum_{j=1}^R \left[ \frac{1}{2^{2j}} \binom{2j+1}{\frac{2j+2}{2}} \alpha_j U^{2j+1} \right] \quad (27)$$

For  $\varepsilon^2$  accuracy, due to the appearance of some cross coupling terms, for instance, the term including  $\alpha_1 \alpha_3$  in Eq. (15), it is much more difficult to find a closed form solution similar to that in Eq. (25). However, using the proposed symbolic computation approach, we have been able to apply  $\varepsilon^2$  DNF analysis for some selected SDOF oscillators and get expressions for the conservative backbone curves, the results can be found in Table A3, Appendix 4.

## 5. Analysis of 2-DOF oscillator with cubic and quintic nonlinearities

In this Section, we consider the two degree-of-freedom oscillator shown in Fig. (6), in which the spring forces are governed by both linear and nonlinear terms, and the nonlinear term contains cubic and quintic orders of polynomial nonlinearities. The main purpose of this Section is to show how the type of analysis carried out for SDOF systems can be applied to oscillators of more than one degree-of-freedom. As a result, the system is assumed to be conservative (undamped and unforced), and the corresponding single-mode backbone are computed (e.g. neglecting the resonant cases).

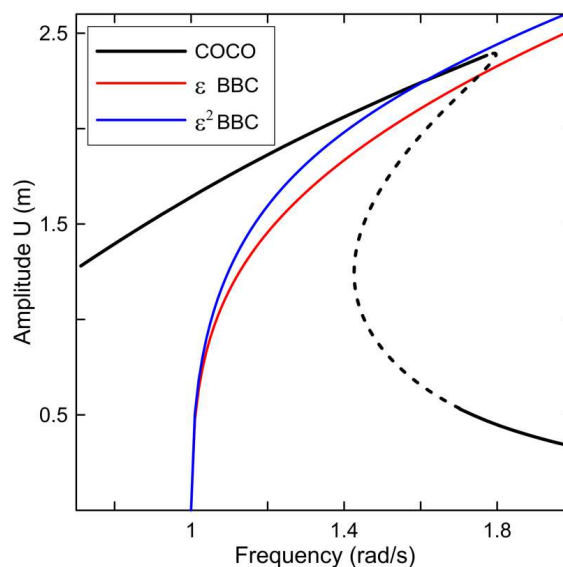


**Fig. 5.** Comparison of DNF results and COCO results for the nonlinear oscillator in Eq. (23), the solid blue and red curves represent the analytical DNF results for  $\varepsilon$  and  $\varepsilon^2$  accuracies, respectively. Moreover, the black line denotes the frequency-response curve computed using COCO; the solid black line shows the stable region of the response while the dashed black line represents the unstable region.

Parameter values are:  $\omega_n = 1$  rad/s, and  $\alpha_1 = \alpha_2 = \alpha_3 = \alpha_4 = 0.1$ .



In matrix form, the system equation of motion can be written as

$$\begin{bmatrix} m & 0 \\ 0 & m \end{bmatrix} \ddot{\mathbf{x}} + \begin{bmatrix} k_1 + k_2 & -k_2 \\ -k_2 & k_1 + k_2 \end{bmatrix} \mathbf{x} + \begin{bmatrix} \kappa_{3,1}x_1^3 - \kappa_{3,2}(x_2 - x_1)^3 + \kappa_{5,1}x_1^5 - \kappa_{5,2}(x_2 - x_1)^5 \\ \kappa_{3,1}x_2^3 + \kappa_{3,2}(x_2 - x_1)^3 + \kappa_{5,1}x_2^5 + \kappa_{5,2}(x_2 - x_1)^5 \end{bmatrix} = \begin{bmatrix} 0 \\ 0 \end{bmatrix} \tag{28}$$

where  $\mathbf{x} = [x_1 \ x_2]^T$  and the two masses are of identical mass  $m$ , and the linear stiffness coefficients are  $k_1$  and  $k_2$ . The nonlinear stiffnesses are denoted by  $\kappa$  with subscripts that reflect both the order of the nonlinearity and the spring number, thus, the cubic stiffness coefficients are  $\kappa_{3,1}$  and  $\kappa_{3,2}$  and the quintic stiffness coefficients are  $\kappa_{5,1}$  and  $\kappa_{5,2}$ , respectively. This form of the subscript is chosen to help generalization of this problem to include higher orders of odd nonlinearities. The analysis of such a system starts by obtaining the linear version of Eq. (28), by setting all the nonlinear stiffnesses to be zero. Following that, the linear modal analysis leads to a modal transformation of

$$\mathbf{x} = \Phi \mathbf{q} \quad \text{where} \quad \Phi = \begin{bmatrix} 1 & 1 \\ 1 & -1 \end{bmatrix}$$

Then, if this linear modal transformation is applied to the nonlinear system in Eq. (28) we obtain the following

$$\ddot{\mathbf{q}} + \begin{bmatrix} \omega_{n1}^2 & 0 \\ 0 & \omega_{n2}^2 \end{bmatrix} \mathbf{q} + \frac{\kappa}{m} \begin{bmatrix} q_1^3 + 3q_1q_2^2 + q_1^5 + 5q_1q_2^4 \\ \gamma_1q_2^3 + 3q_1^2q_2 + \gamma_2q_2^5 + 5q_1^4q_2 \end{bmatrix} = \begin{bmatrix} 0 \\ 0 \end{bmatrix} \tag{29}$$

where  $\omega_{n1}^2 = \frac{k}{m}$ ,  $\omega_{n2}^2 = \frac{3k}{m}$  are the natural frequencies, while  $\gamma_1 = 1 + 8\kappa_{3,2}/\kappa_{3,1}$  and  $\gamma_2 = 1 + 32\kappa_{5,2}/\kappa_{5,1}$ . Now we follow the Step 2 of the DNF procedure for MDOF systems as described in Appendix 1.

Following the DNF procedure (see [9, 14] for details), one can compute approximate analytical expressions for backbone curves. For this system of coupled cubic-quintic oscillators, considering the non-resonant case, where  $\omega_{r2} \neq \omega_{r1}$ , we get the following expressions of the backbone curves

$$U_1 \left\{ \omega_{n1}^2 - \omega_{r1}^2 + \frac{3\kappa_{3,1}}{4m} [U_1^2 + 2U_2^2(2+p)] + \frac{5\kappa_{5,1}}{8m} [U_1^4 + 2U_2^4(2+p)] \right\} = 0 \tag{30a}$$

$$U_2 \left\{ \omega_{n2}^2 - \omega_{r2}^2 + \frac{3\kappa_{3,1}}{4m} [\gamma_1U_2^2 + 2U_1^2(2+p)] + \frac{5\kappa_{5,1}}{8m} [\gamma_2U_2^4 + 2U_1^4(2+p)] \right\} = 0 \tag{30b}$$

where  $p$  denotes two main cases corresponding to the in-unison and out-of-unison cases as follows:

- if  $p = +1$ , we have the in-unison case, where the phase difference  $|\phi_1 - \phi_2| = 0$  for the in-phase case and  $|\phi_1 - \phi_2| = \pm n\pi$ ,  $n = 1, 2, 3, \dots$  which represents the out-of-phase case.
- if  $p = -1$ , we have the out-of-unison case where the phase difference  $|\phi_1 - \phi_2| = \pm \frac{n\pi}{2}$  for  $n = 1, 2, 3, \dots$  which represents the out-of-unison case.

Accordingly, we can consider several cases of the backbone curves, in this work we consider the case of single-mode backbone curves (usually denoted by  $S$ , refer to [14] for more details of the single-mode and double-mode backbone curves). The single-mode backbone curves can be generated when setting  $U_2 = 0$  in Eq. (30a), or  $U_1 = 0$  in Eq. (30b), for which we get

$$S_1 \Rightarrow U_2 = 0 \Rightarrow \omega_{r1}^2 = \omega_{n1}^2 + \frac{3\kappa_{3,1}}{4m} U_1^2 + \frac{5\kappa_{5,1}}{8m} U_1^4, \tag{31a}$$

$$S_2 \Rightarrow U_1 = 0 \Rightarrow \omega_{r2}^2 = \omega_{n2}^2 + \frac{3\kappa_{3,1}}{4m} \gamma_1 U_2^2 + \frac{5\kappa_{5,1}}{8m} \gamma_2 U_2^4 = 0 \tag{31b}$$

In these single-mode backbone curves, no phase coupling occurs between the two modal coordinates,  $u_1$  and  $u_2$ . In order to explore the case of phase coupling between the two modal coordinates, it is possible to consider the in-unison case when  $p = +1$ . In literature, some research has been conducted to study the double-mode (or two mode) modal interactions, see [9] as an example. However, modal-interactions are out of the scope of this work and we only consider the single-mode backbone curves. In Fig. (7) sample results of the single-mode backbone curves for this oscillator are shown.

The key point is to notice the similarity between the single-mode backbone curves for the 2-DOF system, Eq. (31), and the corresponding results of the SDOF cubic-quintic oscillator, Eq. (24). Hence, the single-mode backbone curves, truncated to  $\epsilon$  accuracy, for a 2-DOF nonlinearly couple oscillators with odd polynomial nonlinear stiffness terms, can be written as

$$S_1 \Rightarrow \omega_{r1}^2 = \omega_{n1}^2 + \sum_{j=1}^R \left[ \frac{1}{(2)^{2j}} \left( \frac{2j+1}{2} \right) \kappa_{2j+1,1} U^{2j+1} \right] \tag{32a}$$

$$S_2 \Rightarrow \omega_{r2}^2 = \omega_{n2}^2 + \sum_{j=1}^R \left[ \frac{1}{(2)^{2j}} \left( \frac{2j+1}{2} \right) \kappa_{2j+1,1} \gamma_j U^{2j+1} \right] \tag{32b}$$

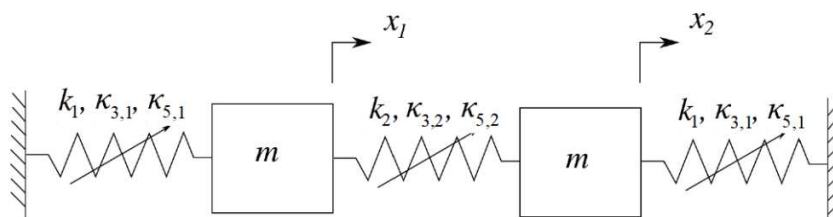


Fig. 6. The schematic diagram of the 2-DOF cubic-quintic oscillator in Section 5.



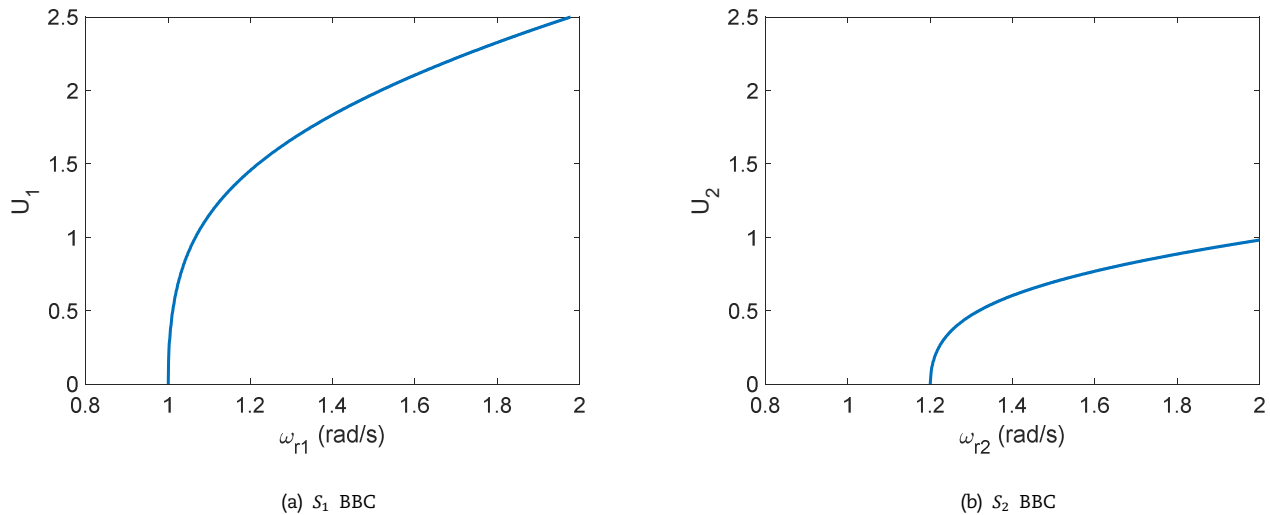


Fig. 7. Single-mode backbone curves of the 2-DOF oscillator studied in Section 5: (a)  $S_1$  backbone curve which represents the projection of  $U_1$  against  $\omega_{r1}$ , (b)  $S_2$  backbone curve which represents the projection of  $U_2$  against  $\omega_{r2}$ . Parameter values are:  $\omega_{n1} = 1$  rad/s,  $\omega_{n2} = 1.2$  rad/s and  $\kappa_{3,1} = \kappa_{3,2} = \kappa_{5,1} = \kappa_{5,2} = 0.1$ .

where  $\gamma_j = 1 + (2)^{2j+1} \left( \frac{\kappa_{2j+1,2}}{\kappa_{2j+1,1}} \right)$ . Using Eq. (32), the single-mode backbone curves of the 2-DOF oscillator with odd polynomial nonlinearities can be computed. This example shows how (at least for the relatively simple case of single mode backbone curves) the analysis for cubic-quintic SDOF oscillators relates to the 2-DOF case.

## 6. Conclusion

In this paper, the direct normal forms method has been used to study nonlinear oscillators with higher order polynomial stiffness nonlinear terms. For the SDOF case, the analysis has been performed for two orders of series expansion,  $\varepsilon$  and  $\varepsilon^2$ , and the related backbone curves were derived for both of cases. The results were compared with a selection of other methods already available in the published literature. One point of interest was that in the case of only odd nonlinear terms (like the cubic-quintic) the  $\varepsilon^2$  order solutions were not always more accurate than the  $\varepsilon$  order solutions (when compared to the benchmark case). When even nonlinear terms were added, as with the generic cubic-quintic SDOF oscillator this changed, and here the  $\varepsilon^2$  order solutions were always more accurate than the  $\varepsilon$  order solutions – as would be expected. In addition, it was shown that, for the SDOF oscillators considered with only odd nonlinear terms, the expression for the backbone curve of the system to  $\varepsilon$  order could be generalized. This was not the case when even nonlinearities were present and in this case  $\varepsilon^2$  accuracy was needed. In terms of methodology, the use of symbolic computations helped deal with algebraic complexity, for the higher orders nonlinearities and/or degrees of freedom. As a final example of the paper, a two degree-of-freedom cubic-quintic oscillator was considered. Here it was shown that for single mode backbone curves (ignoring potential resonances and out-of-unison responses) there was a similar structure in the approximate expressions for the backbone curves when compared with the equivalent SDOF cubic-quintic cases. This demonstrates that a possible general relationship exists for SDOF and MDOF oscillators of this type, at least in the simplest cases. This may be a worthwhile topic for future research.

## Author Contributions

A. Nasir carried out the symbolic computations, analytical derivations, and the numerical simulation work. N. Sims edited the manuscript and contributed to the analysis of the nonlinear oscillators. D. Wagg edited the manuscript and developed some of the underlying novel concepts for this work.

## Acknowledgments

Ayman Nasir has a scholarship funded by Alzaytoonah University of Jordan in order to obtain his PhD degree. The authors would also like to thank Nour Atieh for useful discussions regarding this work. Moreover, the authors highly appreciate the reviewers' contribution, particularly, the contribution of the anonymous reviewer who pointed out the result appearing in Eq. (26).

## Conflict of Interest

The authors declared no potential conflicts of interest with respect to the research, authorship, and publication of this article.

## Funding

Ayman Nasir has a scholarship funded by Alzaytoonah University of Jordan. Apart from this, the authors received no other financial support for the research.

## References

- [1] Xin Z.F., Neild S.A., Wagg D.J., and Zuo Z.X., Resonant response functions for nonlinear oscillators with polynomial type nonlinearities, *Journal of Sound and Vibration*, 332 (7) 2013, 1777–1788.



- [2] Wang S. and Huseyin K., 'Maple' Analysis of nonlinear oscillations, *Mathematical and Computer Modelling*, 16(11), 1992, 49-57.
- [3] Bellizzi S. and Bouc R., A new formulation for the existence and calculation for nonlinear normal modes, *Journal of Sound and Vibration*, 287(3), 2005, 545-569.
- [4] Shaw A.D., Neild S.A., and Wagg D.J., Dynamic analysis of high static low dynamic stiffness vibration isolation mounts, *Journal of Sound and Vibration*, 332, 2012, 1437-1455.
- [5] Jezequel L. and Lamarque, C. H., Analysis of nonlinear dynamic systems by the normal form theory, *Journal of Sound and Vibration*, 149(3), 1991, 429-459.
- [6] Suleman M. and Wu Q., Comparative solution of nonlinear quintic cubic oscillator using modified homotopy method, *Advances in Mathematical Physics*, 2015, Article ID 932905, 1-5.
- [7] Razzak M.A., An analytical approximate technique for solving cubic-quintic Duffing oscillator, *Alexandria Engineering Journal*, 55, 2016, 2959-2965.
- [8] Alexander N.A. and Schilder, F., Exploring the performance of a nonlinear tuned mass damper, *Journal of Sound and Vibration*, 319(1-2), 2009, 445-462.
- [9] Cammarano A., Hill T.L., Neild S.A., and Wagg D.J., Bifurcations of backbone curves for systems of coupled nonlinear two mass oscillator, *Nonlinear Dynamics*, 77(1-2), 2014, 311-320.
- [10] Lai S.K., Lim C.W., Wu B.S., Wang C., Zeng Q.C. and He X.F., Newton-harmonic balancing approach for accurate solutions to nonlinear cubic-quintic Duffing oscillator, *Applied Mathematical Modelling*, 33(2), 2009, 852-866.
- [11] Liu X., Wagg, D. J.,  $\varepsilon^2$ -order normal form analysis for a two-degree-of-freedom nonlinear coupled oscillator, *Nonlinear Dynamics of Structures, Systems and Devices*, Springer, 2020, 25-33.
- [12] Hale J.K., *Oscillations in nonlinear systems*, McGraw-Hill, 1963.
- [13] Urabe M., *Nonlinear autonomous oscillations: Analytical theory*, Volume 34, Academic Press, 1967.
- [14] Wagg D.J., Neild S.A., *Nonlinear vibration with control: for flexible and adaptive structures*, Solid Mechanics and its Applications, 2nd edition, vol. 218, Springer, Berlin, Germany, 2014.
- [15] Nayfeh A.H., Mook D., *Nonlinear oscillations*, Wiley, New York, 1995.
- [16] Nayfeh A.H., *Introduction to Perturbation Techniques*, John Wiley and Sons, New York, 1981.
- [17] Schilder F., Dankowicz H., *Recipes for Continuation*, SIAM Computational Science and Engineering, 2013.
- [18] Schilder F., Dankowicz H., *Continuation core and toolboxes (coco)*. Available at: <https://sourceforge.net/projects/cocotools/>, 2017.
- [19] Thomsen J., *Vibrations and Stability: Order and Chaos*, McGraw Hill, 1997.
- [20] Richards D., *Advanced mathematical methods with Maple*, Cambridge University Press, 2009.
- [21] Enns R., McGuire G., *Nonlinear physics with Maple for scientists and engineers*, Springer, 2000.
- [22] Kovacic I., Brennan M.J., *The Duffing Equation: Nonlinear Oscillators and their Behavior*, John Wiley & Sons, 2011.
- [23] Nayfeh A.H., *The Method of normal forms*, Wiley, New York, 1993.
- [24] Kahn P.B., Zarmi Y., *Nonlinear dynamics: Exploration through normal forms*, Dover Publications, New York, USA, 2014.
- [25] Arnold V.I., *Geometrical methods in the theory of ordinary differential equations*, vol. 250, Springer Science & Business Media, 2012.
- [26] Lui X., *Symbolic Tools for the Analysis of nonlinear dynamical systems*, PhD thesis, Department of Applied Mathematics, University of Western Ontario, London, 1999.
- [27] Hill T.L., Cammarano A., Neild A. and Wagg D.J., An analytical method for the optimization of weakly nonlinear systems, *Proceedings of EURO-DYN 2014*, 2014, 1981-1988.
- [28] Breunung T. and Haller G., Explicit backbone curves from spectral submanifolds of forced-damped nonlinear mechanical systems, *Proceedings of Royal Society A*, 474, 2018, 2018-0083.

## APPENDICES

### Appendix 1: Summary of the DNF procedure for conservative systems

Considering a general unforced, nonlinear,  $N$ -degree-of-freedom mechanical system, whose equation of motion may be written as

$$\mathbf{M}\ddot{\mathbf{x}} + \mathbf{K}\mathbf{x} + \varepsilon\mathbf{N}_x(\mathbf{x}) = 0, \quad (\text{A.1})$$

where  $\mathbf{x}$  is an  $\{N \times 1\}$  vector of physical displacements,  $\mathbf{M}$  and  $\mathbf{K}$  are  $\{N \times N\}$  matrices of mass and linear stiffness respectively,  $\mathbf{N}_x(\mathbf{x})$  is an  $\{N \times 1\}$  vector of stiffness related nonlinear terms and  $\varepsilon$  is used to denote smallness of the nonlinear terms. Here, for the application of the direct normal form technique, the nonlinear terms are assumed to be able to be expressed in a polynomial form in terms of  $\mathbf{x}$ .

The first step of the direct normal form technique is the linear modal transform to decouple the linearly coupled terms, which is written as

$$\mathbf{x} = \Phi\mathbf{q}, \quad (\text{A.2})$$

and the resulting equation of motion in modal coordinates is

$$\ddot{\mathbf{q}} + \Lambda\mathbf{q} + \varepsilon\mathbf{N}_q(\mathbf{q}) = 0, \quad (\text{A.3})$$

where  $\mathbf{q}$  is  $\{N \times 1\}$  vector of linear modal displacement and  $\Phi$  is an  $\{N \times N\}$  matrix of linear mode shape matrix, and  $\Lambda$  is an  $\{N \times N\}$  diagonal matrix of the square of natural frequencies, which can be found from the eigenvalues problem  $\Phi\Lambda = \mathbf{M}^{-1}\mathbf{K}\Phi$ , then the nonlinear terms vector becomes

$$\varepsilon\mathbf{N}_q(\mathbf{q}) = \varepsilon\Phi^{-1}\mathbf{M}^{-1}\mathbf{N}_x(\Phi\mathbf{q}), \quad (\text{A.4})$$

The following step of the direct normal form technique is the nonlinear near-identity transformation, i.e.

$$\mathbf{q} = \mathbf{u} + \varepsilon\mathbf{H}(\mathbf{u}), \quad (\text{A.5})$$

which results in a resonant equation of motion, written as

$$\ddot{\mathbf{u}} + \Lambda\mathbf{u} + \varepsilon\mathbf{N}_u(\mathbf{u}) = 0, \quad (\text{A.6})$$

where  $\mathbf{u}$  and  $\mathbf{H}(\mathbf{u})$  are the fundamental and harmonic components of  $\mathbf{q}$  respectively, and  $\mathbf{N}_u(\mathbf{u})$  is an  $\{N \times 1\}$  vector of resonant nonlinear terms.

To determine the resonant nonlinear terms, the vectors  $\mathbf{N}_u(\mathbf{u})$  and  $\mathbf{H}(\mathbf{u})$  are expressed in a series form as,



$$\varepsilon \mathbf{N}_u(\mathbf{u}) = \varepsilon \mathbf{n}_{u(1)}(\mathbf{u}) + \varepsilon^2 \mathbf{n}_{u(2)}(\mathbf{u}) + \dots \tag{A.7a}$$

$$\varepsilon \mathbf{H}(\mathbf{u}) = \varepsilon \mathbf{h}_{(1)}(\mathbf{u}) + \varepsilon^2 \mathbf{h}_{(2)}(\mathbf{u}) + \dots, \tag{A.7b}$$

and  $\mathbf{N}_q(\mathbf{q})$  is expanded in a Taylor series about the equilibrium  $q = u$ , written as

$$\varepsilon \mathbf{N}_q(\mathbf{q}) = \varepsilon \mathbf{N}_q(\mathbf{u}) + \varepsilon^2 \frac{\partial}{\partial \mathbf{u}} \mathbf{N}_q(\mathbf{u}) \mathbf{H}(\mathbf{u}) + \dots, \tag{A.8}$$

Additionally, a frequency detuning expression is introduced, based on the that the response frequencies of nonlinear systems are often distinct from their natural frequencies, written as,

$$\mathbf{\Lambda} = \mathbf{\Gamma} + \varepsilon \mathbf{\Delta}, \tag{A.9}$$

where  $\mathbf{\Gamma}$  is an  $\{N \times N\}$  diagonal matrix of square of resonant frequencies, and  $\mathbf{\Delta} = \mathbf{\Lambda} - \mathbf{\Gamma}$ . Now, substituting Eqs. (A7), (A8) and (A9) into Eq. (A3) to compare with Eq. (A6) gives,

$$\varepsilon \frac{d^2}{dt^2} \mathbf{h}_{(1)}(\mathbf{u}) + \varepsilon^2 \frac{d^2}{dt^2} \mathbf{h}_{(2)}(\mathbf{u}) + \varepsilon \mathbf{\Gamma} \mathbf{h}_{(1)}(\mathbf{u}) + \varepsilon^2 \mathbf{\Delta} \mathbf{h}_{(1)}(\mathbf{u}) + \varepsilon^2 \mathbf{\Lambda} \mathbf{h}_{(2)}(\mathbf{u}) + \varepsilon \mathbf{N}_q(\mathbf{u}) + \varepsilon^2 \frac{\partial}{\partial \mathbf{u}} \mathbf{N}_q(\mathbf{u}) \mathbf{h}_{(1)}(\mathbf{u}) + \dots = \varepsilon \mathbf{n}_{u(1)}(\mathbf{u}) + \varepsilon^2 \mathbf{n}_{u(2)}(\mathbf{u}) + \dots, \tag{A.10}$$

this leads to expressions that must be balanced in the following order

$$\varepsilon^1: \frac{d^2}{dt^2} \mathbf{h}_{(1)}(\mathbf{u}) + \mathbf{\Gamma} \mathbf{h}_{(1)}(\mathbf{u}) + \mathbf{n}_{(1)}(\mathbf{u}) = \mathbf{n}_{u(1)}(\mathbf{u}) \tag{A.11a}$$

$$\varepsilon^2: \frac{d^2}{dt^2} \mathbf{h}_{(2)}(\mathbf{u}) + \mathbf{\Gamma} \mathbf{h}_{(2)}(\mathbf{u}) + \mathbf{n}_{(2)}(\mathbf{u}) = \mathbf{n}_{u(2)}(\mathbf{u}) \tag{A.11b}$$

where,

$$\mathbf{n}_{(1)}(\mathbf{u}) = \mathbf{N}_q(\mathbf{u}) \tag{A.12a}$$

$$\mathbf{n}_{(2)}(\mathbf{u}) = (\mathbf{\Lambda} - \mathbf{\Gamma}) \mathbf{h}_{(1)}(\mathbf{u}) + \frac{\partial}{\partial \mathbf{u}} \mathbf{N}_q(\mathbf{u}) \mathbf{h}_{(1)}(\mathbf{u}) \tag{A.12b}$$

Here, an assumed solution of the form

$$u_n = u_{pn} + u_{mn} = \left(\frac{U_n}{2} e^{-i\varphi_n}\right) e^{i\omega_{rn}t} + \left(\frac{U_n}{2} e^{i\varphi_n}\right) e^{-i\omega_{rn}t}, \tag{A.13}$$

is adopted, where  $n = 1, \dots, N, U_n, \varphi_n$  and  $\omega_n$  are the displacement amplitude, phase lag, and response frequency of the  $n$ th mode, respectively. Substituting Eq. (13), the vectors  $\mathbf{n}_{(j)}$ ,  $\mathbf{n}_{(j)}$  and  $\mathbf{n}_{u(j)}$  may all be expressed in terms of a  $\{\mathfrak{I}_j \times 1\}$  vector of nonlinear terms in the original problem, i.e. in  $\mathbf{n}_{(j)}$ . For example, if  $\mathbf{n}_{(j)} = [n_{(j)}] \mathbf{u}_{(j)}^*$  is defined, then by mirroring this structure,  $\mathbf{h}_{(j)} = [h_{(j)}] \mathbf{u}_{(j)}$  and  $\mathbf{n}_{u(j)} = [n_{u(j)}] \mathbf{u}_{(j)}^*$  are obtained, where  $[\bullet]$  denotes a  $\{N \times \mathfrak{I}_j\}$  coefficient matrix. For the case of polynomial nonlinear terms under consideration, then the elements in  $\mathbf{u}_{(j)}^*$  may be written as

$$u_{(j)\ell}^* = \prod_{n=1}^N u_{pn}^{s_{pj,\ell,n}} u_{mn}^{s_{mj,\ell,n}} \tag{A.14}$$

where  $s_{pj,\ell,n}$  and  $s_{mj,\ell,n}$  are exponents of  $u_{pn}$  and  $u_{mn}$  in any element of  $\mathbf{u}_{(j)}^*$  respectively. In order to identify the resonant nonlinear terms retained in  $\mathbf{n}_{u(j)}$  from  $\mathbf{n}_{(j)}$ ,  $\beta_{(j)}$ , is introduced, i.e.

$$\beta_{(j)n,\ell} = \left[ \sum_{n=1}^N (s_{pj,\ell,n} - s_{mj,\ell,n}) \omega_{rn} \right]^2 - \omega_{rn}^2 \tag{A.15}$$

accompanied with the corresponding criteria that

$$\text{Non-resonant: } \beta_{(j)n,\ell} \neq 0, [n_{u(j)}]_{n,\ell} = 0, [h_{(j)}]_{n,\ell} = \frac{[n_{(j)}]_{n,\ell}}{\beta_{(j)n,\ell}}, \tag{A.16a}$$

$$\text{Resonant: } \beta_{(j)n,\ell} = 0, [n_{u(j)}]_{n,\ell} = [n_{(j)}]_{n,\ell}, [h_{(j)}]_{n,\ell} = 0 \tag{A.16b}$$

Once the resonant nonlinear terms are determined to a specific accuracy level, i.e.  $\varepsilon^j$ , with the substitutions of Eq. (A.13), Eq. (A.6) can be written in the form,

$$\chi_n e^{i\omega_{rn}t} + \tilde{\chi}_n e^{-i\omega_{rn}t} = 0, \tag{A.17}$$



**Algorithm:**  $\varepsilon$ -order DNF technique (Non-resonant case) using symbolic computations

**Inputs:** Mass matrix  $M$ , Linear stiffness matrix  $K$ , nonlinear and linear damping vector  $N_x$ , forcing amplitude matrix  $P_x$  and forcing frequency  $\Omega$ .

**Outputs:** Displacement response  $x$ , backbone relations.

**Procedure:**

- *Linear modal transformation*
  1. Calculate linear natural frequencies,  $\Lambda$ , and mode shapes  $\Phi$ .
  2. Calculate nonlinear and linear damping terms vector  $N_x$  and forcing amplitudes  $P_q$ .
- *Forcing transformation*
  3. Determine resonant forcing amplitudes  $P_v$ .
  4. Calculate the forcing transform matrix  $e$  (if exists).
  5. Calculate nonlinear and linear damping terms after forcing transformation  $N_v$ .
- *Nonlinear near identity transformation (symbolically)*
  6. Loop #1: perform a loop over DOF, substitute  $x$ 's and their derivatives by corresponding  $u_p$  and  $u_m$  components (using several if clauses inside the loop).
  7. For each equation in  $N_v$ , calculate the number of terms (as vector) then convert to set, and then find the total number of terms for the whole system (unite all terms for all equations and convert to vector again).
  8. Loop #2 (nested): the outer loop over the DOF, and the inner loop over terms number in each equation, determine the nonlinear and linear damping coefficients, and corresponding unique combination of variables  $u^*$  (using if clauses and coefficients commands)
  9. Loop #3 (nested): calculating  $n^*$  matrix for the whole system.
  10. Loop #4 (nested): calculating power indexes  $s_p$  and  $s_m$  for  $u^*$  (whole system) and placing them in Table (or matrix) form.
  11. Check: multiply  $n^*$  by  $u^*$  and subtract initial equations, zeros must be obtained.
  12. Loop #5 (nested): Forming  $\beta$  matrix, for to DOF and then to the total number of terms, use corresponding  $\beta$  equation.
  13. Loop #6 (nested): Calculate coefficients of resonant terms  $n_u^*$ , and of harmonic terms  $h^*$ .
  14. Calculate the resonant nonlinear and linear damping terms by multiplying  $n_u^*$  by  $u^*$ .
- *Finding backbone curves and inverse transformation to find  $x$ .*

where  $\chi_n$  and  $\bar{\chi}_n$  are time-independent complex conjugates and, finally setting  $\chi_n = 0$  leads to the backbone curve expressions. With the aid of Maple software, symbolic computations are held in order to reach higher accuracy and involve more complex system analysis; with such software it is possible use normal forms analysis and generate codes for SDOF and MDOF oscillators. Finally, the symbolic implementation of the DNF method is shown in the following algorithm.

**Appendix 2: Summary of the DNF procedure for higher order accuracy**

While in most cases the  $\varepsilon$  truncated solution yields acceptable results (compared to numerical solutions), sometimes it can be beneficial (or even required) to extend the analysis to a higher order accuracy. In this section, a brief formulation to  $\varepsilon^2$  accuracy is discussed, more details can be found in [14]. Referring to Eq. (A.10), it is possible to obtain the  $\varepsilon^2$  accuracy solution by finding the  $h_2(u)$  and  $n_{u2}(u)$  vectors, in analogy to Eq. (A.10) it is possible to write

$$\tilde{n}_2(u) + \Gamma h_2(u) + \frac{d^2}{dt^2} h_2(u) = n_{u2}(u) \tag{A.18}$$

where  $\tilde{n}_2(u) = n_2(u) + (\Lambda - \Gamma)h_1(u) + \frac{d}{du}\{n_1(u)\}h_1(u)$

Herein, more complexity can be clearly noticed regarding the nonlinear term, so it is more difficult to obtain the solution to  $\varepsilon^2$  accuracy. However, according to the system being approximated, it will be shown that rather than being considered as a compromising procedure to improve the accuracy, the need of extending the analysis to  $\varepsilon^2$  highly depends on the orders of the nonlinear terms. In matrix form, and similar to the analysis of  $\varepsilon$ , the following terms can be introduced,

$$\begin{aligned} \tilde{n}_2(u) &= n^+ u^+(u_p, u_m) \\ h_2(u) &= h^+ u^+(u_p, u_m) \\ n_{u2}(u) &= n_u^+ u^+(u_p, u_m) \end{aligned} \tag{A.19}$$

where, for SDOF systems,  $n^+$ ,  $h^+$ ,  $n_u^+$  are row vectors, and  $u^+(u_p, u_m)$  is a column vector, hence, the resulting products will be scalars. The step-by-step analysis is performed exactly as the case of  $\varepsilon$ , and  $\beta^+$  is computed accordingly, [14]. Finally, the near-identity transformation, to  $\varepsilon^2$  order, along with the resulted EOM are found to be,

$$\begin{aligned} q &= u + h^+ u^* + h^+ u^+ \\ \ddot{u} + \Lambda u + n^+ u^* + n_u^+ u^+ &= 0 \end{aligned} \tag{A.20}$$

The same procedure with some additional steps can be followed for forced-damped systems, and for systems studied in the resonant case, refer to [14] for detailed analysis of such systems.



Appendix 3: Matrix manipulation for the cubic-quintic nonlinear oscillator

Table A1.  $\varepsilon^2$  DNF matrix results for the cubic-quintic oscillators

$u_l^*$	$\beta_l^*$	$n_{u,l}^*$	$h_l^*$	$u_l^*$	$\beta_l^*$	$n_{u,l}^*$	$h_l^*$
$u_m^3$	$8\omega_r^2$	0	$\frac{\alpha_1(\omega_n^2 - \omega_r^2)}{64\omega_r^4}$	$u_p^2 u_m^7$	$24\omega_r^2$	0	$\frac{55\alpha_2^2}{96\omega_r^6}$
$u_m^5$	$24\omega_r^2$	0	$\frac{9\alpha_1^2 + \alpha_2(\omega_n^2 - \omega_r^2)}{576\omega_r^6}$	$u_p^3 u_m^5$	0	$\frac{3\alpha_1^2}{8\omega_r^2}$	0
$u_m^7$	$48\omega_r^2$	0	$\frac{\alpha_1\alpha_2}{64\omega_r^4}$	$u_p^3 u_m^4$	0	$\frac{5\alpha_1\alpha_2}{\omega_r^2}$	0
$u_m^9$	$80\omega_r^2$	0	$\frac{\alpha_2^2}{384\omega_r^4}$	$u_p^3 u_m^6$	$8\omega_r^2$	0	$\frac{235\alpha_2^2}{96\omega_r^4}$
$u_p^3$	$8\omega_r^2$	0	$\frac{\alpha_1(\omega_n^2 - \omega_r^2)}{64\omega_r^4}$	$u_p^4 u_m$	$8\omega_r^2$	0	$\frac{6\alpha_1^2 + 5\alpha_2(\omega_n^2 - \omega_r^2)}{64\omega_r^4}$
$u_p^5$	$24\omega_r^2$	0	$\frac{9\alpha_1^2 + \alpha_2(\omega_n^2 - \omega_r^2)}{576\omega_r^6}$	$u_p^4 u_m^3$	0	$\frac{5\alpha_1\alpha_2}{\omega_r^2}$	0
$u_p^7$	$48\omega_r^2$	0	$\frac{\alpha_1\alpha_2}{64\omega_r^4}$	$u_p^4 u_m^5$	0	$\frac{95\alpha_2^2}{6\omega_r^2}$	0
$u_p^9$	$80\omega_r^2$	0	$\frac{\alpha_2^2}{384\omega_r^4}$	$u_p^5 u_m^2$	$8\omega_r^2$	0	$\frac{61\alpha_1\alpha_2}{64\omega_r^4}$
$u_p u_m^4$	$8\omega_r^2$	0	$\frac{6\alpha_1^2 + 5\alpha_2(\omega_n^2 - \omega_r^2)}{64\omega_r^4}$	$u_p^5 u_m^4$	0	$\frac{95\alpha_2^2}{6\omega_r^2}$	0
$u_p u_m^6$	$24\omega_r^2$	0	$\frac{37\alpha_1\alpha_2}{192\omega_r^4}$	$u_p^6 u_m$	$24\omega_r^2$	0	$\frac{37\alpha_1\alpha_2}{192\omega_r^4}$
$u_p u_m^8$	$48\omega_r^2$	0	$\frac{95\alpha_2^2}{1152\omega_r^4}$	$u_p^6 u_m^3$	$8\omega_r^2$	0	$\frac{235\alpha_2^2}{96\omega_r^4}$
$u_p^2 u_m^3$	0	$\frac{3\alpha_1^2}{8\omega_r^2}$	0	$u_p^7 u_m^2$	$24\omega_r^2$	0	$\frac{55\alpha_2^2}{96\omega_r^4}$
$u_p^2 u_m^5$	$8\omega_r^2$	0	$\frac{61\alpha_1\alpha_2}{64\omega_r^4}$	$u_p^8 u_m^1$	$48\omega_r^2$	0	$\frac{95\alpha_2^2}{1152\omega_r^4}$

Appendix 4: Some results obtained for different types of oscillators

Table A2. Backbone curves of SDOF oscillators with polynomial nonlinear term truncated to  $\varepsilon$  and  $\varepsilon^2$  accuracies

Nonlinear vector	$\varepsilon$ Backbone curve	$\varepsilon^2$ Backbone curve
$\alpha x^2(t)$	$\omega_n^2$	$\omega_n^2 - \frac{5}{6\omega_r^2} \alpha^2 U^2$
$\alpha x^3(t)$	$\omega_n^2 + \frac{3}{4} \alpha U^2$	$\omega_n^2 + \frac{3}{4} \alpha U^2 + \frac{3}{128\omega_r^2} \alpha^2 U^4$
$\alpha x^4(t)$	$\omega_n^2$	$\omega_n^2 - \frac{63}{80\omega_r^2} \alpha^2 U^6$
$\alpha x^5(t)$	$\omega_n^2 + \frac{5}{8} \alpha U^4$	$\omega_n^2 + \frac{5}{8} \alpha U^4 + \frac{95}{1536\omega_r^2} \alpha^2 U^8$
$\alpha x^6(t)$	$\omega_n^2$	$\omega_n^2 - \frac{1287}{1792\omega_r^2} \alpha^2 U^{10}$
$\alpha x^7(t)$	$\omega_n^2 + \frac{35}{64} \alpha U^6$	$\omega_n^2 + \frac{35}{64} \alpha U^6 + \frac{6405}{65536\omega_r^2} \alpha^2 U^{12}$
$\alpha x^8(t)$	$\omega_n^2$	$\omega_n^2 - \frac{12155}{18432\omega_r^2} \alpha^2 U^{14}$
$\alpha x^9(t)$	$\omega_n^2 + \frac{36}{128} \alpha U^8$	$\omega_n^2 + \frac{63}{128} \alpha U^8 + \frac{84393}{655360\omega_r^2} \alpha^2 U^{16}$
$\alpha x^{10}(t)$	$\omega_n^2$	$\omega_n^2 - \frac{440895}{720896\omega_r^2} \alpha^2 U^{18}$
$\alpha x^{11}(t)$	$\omega_n^2 + \frac{231}{512} \alpha U^{10}$	$\omega_n^2 + \frac{231}{512} \alpha U^{10} + \frac{1955107}{12582912\omega_r^2} \alpha^2 U^{20}$
$\alpha x^{12}(t)$	$\omega_n^2$	$\omega_n^2 - \frac{3900225}{6815744\omega_r^2} \alpha^2 U^{22}$
$\alpha x^{13}(t)$	$\omega_n^2 + \frac{429}{1024} \alpha U^{12}$	$\omega_n^2 + \frac{429}{1024} \alpha U^{12} + \frac{20941713}{117440512\omega_r^2} \alpha^2 U^{24}$
$\alpha x^{14}(t)$	$\omega_n^2$	$\omega_n^2 - \frac{4524261}{8388608\omega_r^2} \alpha^2 U^{26}$
$\alpha x^{15}(t)$	$\omega_n^2 + \frac{6435}{16384} \alpha U^{14}$	$\omega_n^2 + \frac{6435}{16384} \alpha U^{14} + \frac{1703280825}{8589934592\omega_r^2} \alpha^2 U^{28}$

Table A3. Backbone curves of  $\varepsilon^2$  accuracy for SDOF oscillators with combined polynomial nonlinear term truncated


Nonlinear vector	$\varepsilon^2$ Backbone curve
$\alpha_1 x^2(t) + \alpha_2 x^3(t)$	$\omega_n^2 + \frac{3}{128\omega_r^2} \alpha_2^2 U^4 + \frac{3}{4} \alpha_2 U^2 - \frac{5}{6\omega_r^2} \alpha^2 U^2$
$\alpha_1 x^2(t) + \alpha_2 x^4(t)$	$\omega_n^2 - \frac{63}{80\omega_r^2} \alpha_2^2 U^6 - \frac{7}{4\omega_r^2} \alpha_1 \alpha_2 U^4 - \frac{5}{6\omega_r^2} \alpha_1^2 U^2$
$\alpha_1 x^2(t) + \alpha_2 x^5(t)$	$\omega_n^2 + \frac{95}{1536\omega_r^2} \alpha_2^2 U^8 + \frac{5}{8} \alpha_2 U^4 - \frac{5}{6\omega_r^2} \alpha^2 U^2$
$\alpha_1 x^2(t) + \alpha_2 x^6(t)$	$\omega_n^2 - \frac{1287}{1792\omega_r^2} \alpha_2^2 U^{10} - \frac{15}{8\omega_r^2} \alpha_1 \alpha_2 U^6 - \frac{5}{6\omega_r^2} \alpha_1^2 U^2$
$\alpha_1 x^2(t) + \alpha_2 x^7(t)$	$\omega_n^2 + \frac{6405}{65536\omega_r^2} \alpha_2^2 U^{12} + \frac{35}{64} \alpha_2 U^6 - \frac{5}{6\omega_r^2} \alpha^2 U^2$






$$\begin{array}{l}
 \alpha_1 x^2(t) + \alpha_2 x^8(t) \\
 \alpha_1 x^2(t) + \alpha_2 x^9(t) \\
 \alpha_1 x^3(t) + \alpha_2 x^4(t) \\
 \alpha_1 x^3(t) + \alpha_2 x^5(t) \\
 \alpha_1 x^2(t) + \alpha_2 x^3(t) + \alpha_3 x^5(t) \\
 \alpha_1 x^2(t) + \alpha_2 x^3(t) + \alpha_3 x^4(t) + \\
 \alpha_4 x^5(t) + \alpha_5 x^6(t)
 \end{array}
 \begin{array}{l}
 \omega_n^2 - \frac{12155}{18432\omega_f^2} \alpha_2^2 U^{14} - \frac{385}{192\omega_f^2} \alpha_1 \alpha_2 U^8 - \frac{5}{6\omega_f^2} \alpha_1^2 U^2 \\
 \omega_n^2 + \frac{84393}{655360\omega_f^2} \alpha_2^2 U^{16} + \frac{63}{128} \alpha_2 U^8 - \frac{5}{6\omega_f^2} \alpha_1^2 U^2 \\
 \omega_n^2 - \frac{63}{80\omega_f^2} \alpha_2^2 U^6 + \frac{3}{128\omega_f^2} \alpha_1^2 U^4 + \frac{3}{4} \alpha_1 U^2 \\
 \omega_n^2 + \frac{3}{4} \alpha_1 U^2 + \frac{5}{8} \alpha_2 U^4 + \frac{3}{128\omega_f^2} \alpha_1^2 U^4 + \frac{5}{64\omega_f^2} \alpha_1 \alpha_2 U^6 + \frac{95}{1536\omega_f^2} \alpha_2^2 U^8 \\
 \omega_n^2 + \frac{3}{4} \alpha_1 U^2 + \frac{5}{8} \alpha_2 U^4 + \frac{3}{128\omega_f^2} \alpha_1^2 U^4 + \frac{5}{64\omega_f^2} \alpha_1 \alpha_2 U^6 + \frac{95}{1536\omega_f^2} \alpha_2^2 U^8 - \frac{5}{6\omega_f^2} \alpha_1^2 U^2 \\
 \omega_n^2 + \frac{3}{4} \alpha_1 U^2 + \frac{5}{8} \alpha_2 U^4 + \frac{3}{128\omega_f^2} \alpha_1^2 U^4 + \frac{5}{64\omega_f^2} \alpha_1 \alpha_2 U^6 + \frac{95}{1536\omega_f^2} \alpha_2^2 U^8 - \frac{5}{6\omega_f^2} \alpha_1^2 U^2 - \frac{1287}{1792\omega_f^2} \alpha_5^2 U^{10} \\
 - \frac{99}{64\omega_f^2} \alpha_5 \alpha_3 U^8 - \frac{15}{8\omega_f^2} \alpha_5 \alpha_1 U^6 - \frac{63}{80\omega_f^2} \alpha_3^2 U^6 - \frac{7}{4\omega_f^2} \alpha_3 \alpha_1 U^4
 \end{array}$$

**ORCID iD**

Ayman Nasir  <https://orcid.org/0000-0002-7092-0238>

Neil Sims  <https://orcid.org/0000-0002-7266-2105>

David Wagg  <https://orcid.org/0000-0002-6292-6736>



© 2021 Shahid Chamran University of Ahvaz, Ahvaz, Iran. This article is an open access article distributed under the terms and conditions of the Creative Commons Attribution-Non Commercial 4.0 International (CC BY-NC 4.0 license) (<http://creativecommons.org/licenses/by-nc/4.0/>).

**How to cite this article:** Nasir A., Sims N., Wagg D. Direct Normal Form Analysis of Oscillators with Different Combinations of Geometric Nonlinear Stiffness Terms, *J. Appl. Comput. Mech.*, 7(SI), 2021, 1167–1182. <https://doi.org/10.22055/JACM.2021.34016.2324>

**Publisher’s Note** Shahid Chamran University of Ahvaz remains neutral with regard to jurisdictional claims in published maps and institutional affiliations.

